How Quickly Will the Offshore Ecosystem Recover from the 2010 Deepwater Horizon Oil Spill? Lessons Learned from the 1979 Ixtoc-1 Oil Well Blowout

Melissa Rohal[1], Noe Barrera[1], Elva Escobar-Briones[2], Gregg Brooks[4], David Hollander[3], Rebekka Larson[4], Paul A. Montagna[1]*, Marissa Pryor[1], Isabel C. Romero[3], Patrick Schwing[3,4]

[1]Texas A&M University - Corpus Christi, Harte Research Institute for Gulf of Mexico Studies, 6300 Ocean Drive, Unit 5869, Corpus Christi, Texas 78412, USA.
[2]Universidad Nacional Autonoma de Mexico, Instituto de Ciencias del Mar y Limnologia, A.P. 70-305 Ciudad Universitaria, 04510 Mèxico, D.F. MEXICO
[3]University of South Florida, College of Marine Science, 140 7th Ave S., St Petersburg, FL 33701, USA.
[4]Eckerd College, 4200 54th Ave. S. Saint Petersburg, FL, 33711, USA.

*Corresponding author, others listed alphabetically. Phone: 361-825-2040, Email: Paul.Montagna@tamucc.edu

Submitted to: *Ecological Indicators*, Special Issue: SeventIMCO, the 17th International Meiofauna Conference: Meiofauna in a changing world
Submission Date: November 26, 2019
Revision Date: March 25, 2020

22 **ABSTRACT**

23 The Deepwater Horizon (DWH) accident occurred on 20 April 2010 in the Northern Gulf of
24 Mexico and resulted in a deep-sea plume of petroleum hydrocarbons and a marine oiled snow
25 sedimentation and flocculent accumulation (MOSSFA) event. It is hypothesized that recovery
26 will occur when the contaminated sediment is buried below the biologically active zone of 10
27 cm. Recovery rate can be inferred from the similar Ixtoc-1 blowout and sub-surface oil release
28 that occurred in the Bay of Campeche, Mexico in 1979 – 1980. In 2015, sediment chemistry
29 effects from the Ixtoc-1 were found at 2.4– 2.8 cm sediment depth at stations within 81 and 273
30 km away. Trends of total polycyclic aromatic hydrocarbon concentration, macrofauna family-
31 level diversity, and the nematode to copepod ratio with sediment depth supports the
32 interpretation that the benthic community has not yet recovered from the Ixtoc-1 spill. Based on
33 a sedimentation rate of 0.072 cm/year, the Ixtoc-1 benthic community will recover in 103 more
34 years beyond 2015. Recovery around the DWH will occur in 50 years based on an average
35 sedimentation rate of 0.2 cm/year. These rates demonstrate that benthic recovery in the deep sea
36 is very slow.

37 Keywords: Deepwater Horizon; Meiofauna; Macrofauna; Ixtoc; Oil Spill

38 **1. Introduction**

39 On 20 April 2010, the Deepwater Horizon (DWH) accident occurred in the northern Gulf
40 of Mexico at a water depth of 1525 meters. The benthic community was potentially exposed to
41 an estimated 3.19 million barrels of oil residues (DWH Natural Resource trustees, 2016; Romero
42 et al., 2017). Of all the oil released, up to 35% of the hydrocarbons were suspended in a deep-
43 water plume that later is believed to have settled on the seafloor (Ryerson et al., 2012; Valentine
44 et al., 2014; Romero et al., 2015; Romero et al., 2017). The formation of a Marine Oil Snow

45 Sedimentation and Flocculent Accumulation event (MOSSFA) was observed as the result of the
46 plankton and microorganisms stress responses to petroleum and dispersant exposure (Passow et
47 al., 2012; Ziervogel et al. 2012; Passow, 2016; Daly et al., 2016). This resulted in increased
48 concentrations of oil-residues in the deep-sea area with estimates ranging from 3,200 (Valentine
49 et al., 2014) to ~33,000 km^2 (Romero et al., 2015; Schwing et al., 2017B). The impact on the
50 benthic community is still severe with a 54% loss of macrofauna diversity and 38% loss of
51 meiofauna diversity (Montagna et al., 2013). There was no recovery of this with reduced
52 diversity four years after the spill (Reuscher et al., 2017). Based on what is known about deep-
53 sea biology, it was argued that recovery could take many decades (Montagna et al., 2013). The
54 purpose of the present study is to estimate recovery times for the DWH spill.
55 This exposure combination of direct oil residues and MOSSFA was observed during the
56 Ixtoc-1 well blow out in the Bay of Campeche in the southwestern Gulf of Mexico (Jernelöv and
57 Lindén, 1981). On June 3, 1979, in 51 m of water, high pressure build-up caused the Ixtoc-1
58 well to blow out and catch fire (Jernelöv and Lindén, 1981). The platform sank to the seafloor
59 damaging the stack and well casing allowing the oil and gas to mix close to the seafloor
60 (Jernelöv and Lindén, 1981). The spill continued until March 23, 1980 for 290 days resulting in
61 about 475,000 metric tons (≈ 3.3 million barrels) of oil to be released (Jernelöv and Lindén,
62 1981). It was estimated that 1 – 3 million gallons (24 – 71 thousand barrels) of oil impacted the
63 beaches and resided offshore in tar mats (Oil Spill Intelligence Reports, 1980). Oil moved to the
64 north where a MOSSFA event likely occurred over deep-sea sediments (Sun et al. 2015; Vonk et
65 al., 2015). The Ixtoc-1 and DWH oil spill share several similarities. Both spills occurred
66 because of a buildup of high pressure, occurred close to the coast, occurred near important
67 deltaic systems, and large amounts of dispersants were used (Jernelöv, 2010).

Because of the similarities between DWH and Ixtoc-1, the recovery rate of benthos around the location of the Ixtoc-1 accident can provide parameters that could be used to estimate the recovery of the DWH environment. The Gulf of Mexico is considered a large marine ecosystem unit (Yáñez-Arancibia and Day, 2004; Carlisle, 2014), and we do know how the gradients of benthic community structure and diversity are driven by temperature, salinity, depth, latitude, and longitude throughout the Gulf (Schwing et al. 2020b). Two surficial sediment components of the benthic community, the macrofauna and the meiofauna, are often used as indicators of ecosystem health and therefore, are ideal organisms to study. These two groups represent two different size classes of microscopic animals that live on or in the sediment. Macrofauna are the larger of the two groups and are often retained on a 300 µm sieve while meiofauna are retained on 45 µm sieves (Montagna et al., 2017), but in deep-sea studies meiofauna are sometimes retained on 32 µm sieves (Giere, 2009;) or 20 µm sieves (Danovaro 2010). Neither group can easily escape from disturbance because of their small size and relatively sedentary lifestyle. More importantly both groups have been used as indicators of the DWH deep-sea oil spill (Montagna et al., 2013; Baguley et al., 2015; Washburn et al., 2016). The damage of the deep sea surrounding the DWH site was caused by deposition of contaminants to surface sediments and a loss of diversity in the top 0 to 3 cm of the surface sediment (Washburn et al., 2016; Reuscher et al., 2017) Therefore, it is likely that benthic community recovery will occur when fresh, uncontaminated, sediment buries the contaminated sediment. The benthos are restricted to the top 8 to 10 cm of sediment in the Gulf of Mexico (Montagna et al., 2016), so it is likely that about 10 cm of fresh sediment must be deposited before there is complete recovery. It will take time for sediment to accumulate on the sea floor in the northern Gulf of Mexico, but the Ixtoc spill occurred in 1979 and sufficient time has

passed to determine if this hypothesis is true. This hypothesis is tested by measuring the macrofauna and meiofauna community response and chemical contaminants at the Ixtoc-1 oil spill location vertically within the sediment. If there is an effect from the Ixtoc-1 oil spill in the southern Gulf of Mexico, we can then use sedimentation rates to predict recovery time at the DWH site in the northern Gulf of Mexico.

2 Methods

As part of the Center for the Integrated Modeling and Analysis of Gulf Ecosystems (C-IMAGE) II consortium research program, samples were collected from Jul 30th to August 9th, 2015 onboard the Universidad Nacional Autónoma de México's R/V Justo Sierra. Samples were collected with an Oktopus MUC 12-100 multiple corer in areas believed to have been impacted by the Ixtoc-1 oil according to Sun et al. (2015) (Fig. 1). Samples were collected within the fishery exclusion zone, with the closest station located 4 km south of the original Ixtoc-1 well head (Table 1). Three replicate cores with an inner diameter of 9.5 cm were collected from each station and sliced into 0 – 1, 1 – 3, 3 – 5, and 5 – 10 cm depth sections. Each section-sample was preserved in 7% formalin buffered with Borax© for processing in the lab. At each station water profiles with a CTD were collected. Only the deepest CTD measurements, which were at the bottom, were used for dissolved oxygen (DO), salinity, and temperature in the current study.

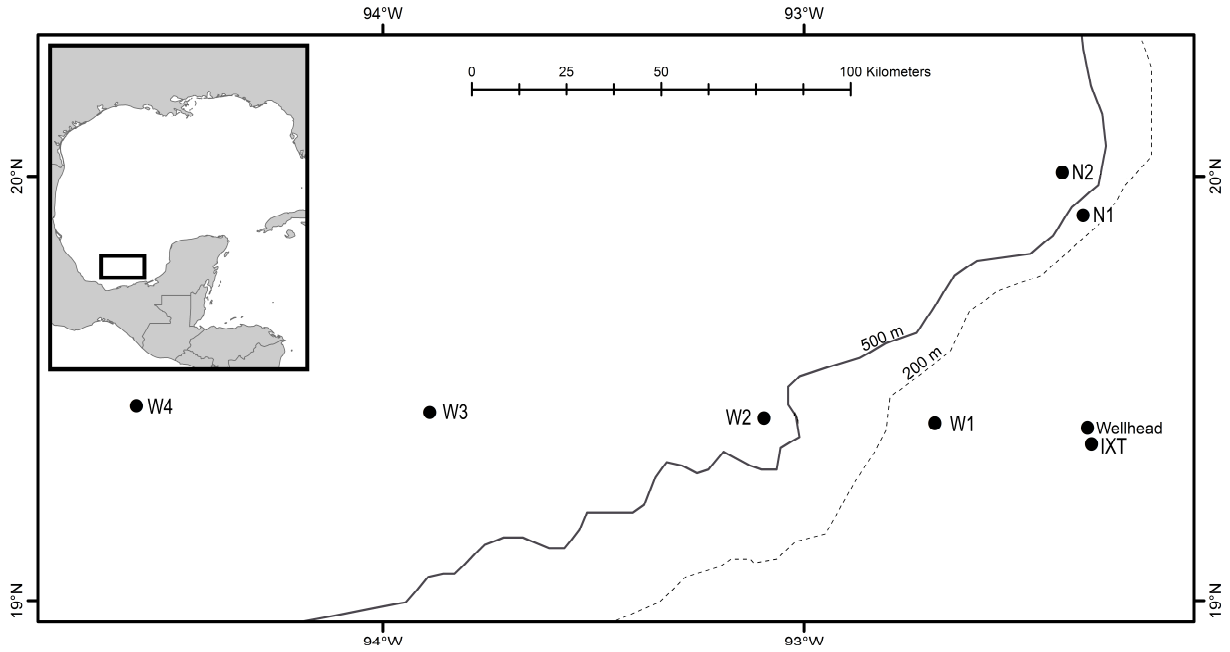

Fig. 1. Map of the sampling stations.

Table 1.

Station location, distance (rounded to the nearest whole number) from the Ixtoc-1 wellhead, and depth.

Station	Latitude (degrees)	Longitude (degrees)	Depth (m)	Distance (km)	Direction	Label
IXTOC1	19.3701	-92.3172	60	4	-	IXT
IXW100	19.4187	-92.6894	179	38	W	W1
IXW250	19.4307	-93.0950	583	81	W	W2
IXW500	19.4442	-93.8887	1010	164	W	W3
IXW750	19.4600	-94.5849	1440	237	W	W4
IXN250	19.9080	-92.3373	779	56	N	N1
IXN500	20.0089	-92.3865	1240	67	N	N2

2.1. Fauna analyses

In the laboratory, the samples were rinsed over stacked 300 µm and 45 µm stacked sieves to separate macrofauna and meiofauna respectively. The first replicate of each station for meiofauna was sorted in its entirety, but this took a week to a month to complete a sample; so the remaining meiofauna replicates were subsampled to complete the analyses within a day or two.

120 The subsamples were separated into equal portions by sediment volumes of 25 or 33%
121 depending on the sediment volume, thus only a portion of replicates 2 – 3 were sorted for each
122 station and section for the meiofauna. The samples were sorted under a dissecting microscope
123 and all macrofauna and metazoan meiofauna were counted and identified. Only the top two
124 sections of the core were sorted, 0 – 1 and 1 – 3 cm, for the meiofauna because that is the
125 sediment depth at which 87% of the meiofauna from 20 cm deep cores are located (Montagna et
126 al., 2017). All macrofauna samples were retained on a 300 µm sieve for the 0 – 1, 1 – 3, 3 – 5,
127 and 5 – 10 cm sections. About 97% of macrofauna occur in the top 10 cm of 20 cm deep cores
128 (Montagna et al. 2017). The sections were sorted and identified to a major taxa level such as
129 phylum, class, or order.

130 **2.2. Geochronology**

131 Long-term preservation of the DWH chemical signal in sedimentary systems has been
132 identified (Romero et al., 2020), which means that it should be possible to identify the Ixtoc-1
133 signal in Bay of Campeche sediments. Short-lived radioisotope geochronologies, based on
134 excess ^{210}Pb ($^{210}Pb_{xs}$) chronological analysis of cores from each station, were used to identify the
135 vertical location within the sediment for the date of 1979-1980 using the methods described in
136 Brooks et al. (2015) and Schwing et al. (2017b). Additional evidence of the Ixtoc-1 signal was
137 measured as Foraminifera calcite stable isotope proxies ($\delta^{13}C_{CaCO3}$) (Schwing and Machain-
138 Castillo, 2020; Schwing et al., 2018) The sediment interval was identified based on three
139 criteria: if depletion of stable carbon in Foraminifera was beyond natural variability, if depletion
140 occurred during 1979-1980, and qualitatively, if the depletions identified as Ixtoc-1 in these
141 cores were the same magnitude (0.3 - 0.4 per mil) as those documented for the three years

following the DWH and which are now preserved below the surface of northern Gulf deep sediments.

2.3. Total polycyclic aromatic hydrocarbons (TPAH) concentrations

Sediment samples were freeze-dried (Labonco® 7754040 vacuum freeze-drier and 7806020 bulk tray) and ground to homogenization (Beriro et al., 2014; Romero et al., 2018). Extraction of samples was done using an Accelerated Solvent Extraction system (ASE 200®, Dionex; temperature: 100°C, pressure: 1500 psi, and solvent mixture of 9:1 (v:v) hexane:dichloromethane). Deuterated surrogate PAHs standards (d_{10}-acenaphthene, d_{10}-phenanthrene, d_{10}-fluoranthene, d_{12}-benz(a)anthracene, d_{12}-benzo(a)pyrene, d_{14}-dibenz(ah)anthracene; Ultra Scientific ISM-750-1) were added to sediment samples prior to extraction. A one-step extraction and clean-up procedure was applied using ~1 g freeze-dried homogenized sample (Romero et al., 2018; Romero, 2019). Sediment extracts were concentrated to ~ 200 µl using a RapidVap (LABONCO RapidVap® Vertex™ evaporator model 73200 series) and a gentle stream of nitrogen. Two extraction control blanks were included with each set of samples (15–20 samples). Prior to GC/MS analysis an internal standard was added to all samples (d_{14}-terphenyl; Ultra Scientific ATS-160-1). All solvents used were at the highest purity available.

One sediment sample was collected at each station, but the samples were split into three pseudoreplicates that were analyzed separately. For analysis of PAHs we followed modified EPA methods 8270D and 8015C, and QA/QC protocols. Analyses were carried in splitless injection mode on an Agilent 7680B gas chromatograph interfaced with an Agilent 7010 triple quadrupole mass spectrometer (GC/MS/MS) using a 30 m RXi-5sil column, UHP helium as the carrier gas, UHP argon gas to facilitate the dissociation of the precursor ions in the collision cell,

and pressure at 1 mTorr, inlet temperature of 295°C, constant flow rate of 1 ml/min, and MS detector temperature at 250°C. GC oven temperature program was 60°C for 2 min, 60°C to 200°C at a rate of 8°C/min, 200°C to 300°C at a rate of 4°C/min and held for 4 min, and 300°C to 325°C at a rate of 10°C/min and held for 5 min. The GC/MS/MS was operated in Multiple Reaction Monitoring mode (MRM). Molecular ion masses for PAHs (precursor and product ions) were selected based on previous studies using GC-MS/MS-MRM (Sorensen et al., 2016; Adhikari et al, 2017; Van enennaam et al., 2018; Romeo et al., 2018). Selected target compounds were: naphthalene and alkylated homologues; acenaphthylene, acenaphthene, fluorene, dibenzothiophene, phenanthrene and anthracene with their alkylated homologues, fluoranthene and pyrene with their alkylated homologues, benz[a]anthracene and chrysene with their alkylated homologues, benzo[b]fluoranthene, benzo[k]fluoranthene, benzo[a]pyrene, dibenz[a,h]anthracene, indeno[1,2,3-cd]pyrene, and benzo[ghi]perylene. For accuracy and precision of analyses we included laboratory blanks for every 10-14 samples, spiked controls for every 15-20 samples, tuned MS/MS to PFTBA (perfluorotributylamine) daily, included daily a standard reference material (NIST 2779). Recovery of individual PAHs ranged within QA/QC criteria of 50–120%. PAH concentrations are reported as recovery corrected. Each PAH analyte was identified using certified standards (Chiron S-4083-K-T, Chiron S-4406-200-T) and performance was checked using a 5-point calibration curve (0.04, 0.08, 0.31, 1.0 ppm). Quantitative determination of PAHs was conducted using response factors (RFs) calculated from the certified standard NIST2779. The limits of quantification (N = 10) ranged from 0.01 to 0.9 ng/g.

186 **2.4. Statistical analyses**

187 Univariate and multivariate analyses were performed using SAS 14.3 and Primer-e
188 version 7 respectively. To correct for sorting subsamples of the meiofauna, abundance for
189 vertical section subsamples was calculated by first averaging the count of each taxa in
190 subsamples from a replicate core and then summing the averages together so that there would be
191 one value per section per replicate. Before analysis all counts were scaled to the number of
192 individuals/m^2. Community metrics of total abundance, Hill's N1 diversity, and richness were
193 calculated for both macrofauna and meiofauna.

194 **2.2.1 Univariate analysis**

195 Univariate analysis of variance (ANOVA) was calculated with PROC GLM in SAS 14.3
196 (SAS, 2017). To test for differences among stations and vertical sediment depths (i.e., sections)
197 the following dependent variables were used: square root transformed total abundance, total
198 polycyclic aromatic hydrocarbons (TPAH), meiofaunal nematode abundance, copepod
199 abundance, and the meiofaunal nematode to copepod ratio (NC). The NC ratio is an indicator of
200 oil pollution at the DWH oil spill site (Montagna et al., 2013; Baguley et al., 2015). To test for
201 differences with sediment depth a two-way partially heirarchical ANOVA was run across
202 stations and sections. Because each replicate was split into sections, each section is from the
203 unique replicates, thus sections are nested within the replicates, but each level of section occurs
204 at each level of station, so these are crossed variable, thus a partially heirarchical design. The
205 replicates are also a random variables, where as the stations and sections are fixed variables, thus
206 a mixed model as well. The statistical model is $Y_{ijk} = \mu + \alpha_j + \beta_{k(j)} + \gamma_l + \alpha\gamma_{jl} + e_{ijkl}$ where Y_{ijk} is
207 the dependent response variable, μ is the overall sample mean, α_j is the main fixed effect for
208 stations, $\beta_{k(j)}$ is the random effect for replicates where k = 1, 2, or 3; γ_l is the main fixed effect for

sections where l = 0– 1, 1– 3, 3– 5,or 5– 10 cm, $\alpha\gamma_{jl}$ is the main fixed effect for the interaction between station and section, and e_{ijkl} is the random error term for each of the i replicate measurements within cells. The correct F-test for stations is to divide mean square of stations by the mean square of the replicates, all other treatments are divded by mean square error. Tukey's Honestly Significant Difference (HSD) test was run as a follow up comparison test. Degree of differences between stastically different samples was calculated by dividing the highest mean by the lowest. Meiofauna and macrofauna were analyzed in separate univariate and multivariate analyses because they are different groups.

2.2.2 Multivariate analysis

Primer-e version 7 software was used to analyze the benthic community by considering the taxonomic groups and the number of individuals (abundance) within each group. To analyze across stations macrofauna and meiofauna were analyzed independently. The abundance data was square root transformed, then a resemblance matrix using Bray-Curtis similarity was created for the following analyses: A hierarchical CLUSTER analysis with group average, a SIMPROF test at a 5% significant level, and 999 permutations. A non-metric multidimensional scaling (nMDS) plot was generated with 1000 restarts and 0.01 minimum stress. A one-way ANOSIM was used to test for differences across stations. To determine which taxonomic group was driving the differences a one-way SIMPER analysis was run on the square root transformed abundance data and Bray-Curtis similarity was used to test for differences across stations and sediment sections.

A principal components analysis (PCA) was run on the environmental variables depth, DO, temperature, salinity, and Total PAHs in SAS 14.3. Prior to analysis, all variables were

231 standardized to a normal distribution with a mean of zero and standard deviation of one so that
232 all variables were on the same scale.

233 **3. Results**

234 **3.1 Station trends**

235 **3.1.1 Environmental**

236 There was little difference in salinity between stations but DO varied by up to 3.24 mg/L
237 and temperature varied by up to 15 °C (Table 2). Chemical analysis of the hydrocarbon
238 concentrations found that TPAH ranged from 43.74 – 156.37 ng/g across stations averaged
239 across the top 10 cm (Table 2). Chronological analysis of benthic foraminifera stable carbon
240 isotopes (Schwing and Machain-Castillo, 2020) identified a signal consistent with Ixtoc between
241 2.4 – 2.8 cm at W2 and from 2.4 – 2.6 cm at W4 (Table 2). A chronological analysis was not
242 possible at stations IXT and W1 because the sediments were mixed and there was no
243 stratification (Table 2). No Ixtoc signal was found at stations W3, N1, and N2.

244 **Table 2. Environmental measurements at each station. Bottom water, and sediment total**
245 **polycyclic aromatic hydrocarbon (TPAH) average total concentration from 0-10 cm. The**
246 **depth of the Ixtoc signal is estimated from values derived from stable carbon isotope**
247 **measurements from benthic Foraminifera (Schwing and Machain-Castillo, 2020).**

Station	Dissolved Oxygen (mg/L)	Temperature (°C)	Salinity (PSU)	TPAH (ng/g)	Depth of Ixtoc Signal
IXT	3.27	19.95	36.43	156.37	Mixed
W1	2.82	15.58	36.04	146.84	Mixed
W2	2.59	8.27	35.03	102.13	2.4 – 2.8 cm
W3	4.05	5.20	34.93	84.73	No Signal
W4	5.61	4.27	34.97	43.74	2.4-2.6 cm
N1	4.02	6.60	34.93	84.86	No Signal
N2	5.83	4.56	34.96	115.60	No Signal

248

249 Total PAH concentrations differed by station ($F_{6,24}$ = 14.96, P = <0.0001) and section
250 (i.e., sediment layer) ($F_{4,24}$ = 7.18, P = 0.0006) (Table 3). TPAH was 4 times higher at station

IXT that was different from all other stations except W1 (Table 3). Section 0 – 1 was higher (up to 1.9 times higher) than sections 5 – 10 and 10 – 20 cm (Table 4).

Table 3. Analysis of variance results for differences among TPAH (ng/g) means by station and section. A) ANOVA table. B) Tukey HSD groupings for TPAH concentrations by station where underlined values are < 0.05. C) Tukey HSD groupings for TPAH concentrations by section.

A)

Source	DF	F Value	Pr > F
Station	6	14.96	<.0001
Section	4	7.18	0.0006

B)

Mean	158.49	136.37	99.83	93.01	78.37	77.65	39.27
Station	IXT	W1	N2	W1	W2	N1	W3

C)

Mean	129	108	98.9	83.6	68.3
Section	0 - 1	3 - 5	1 - 3	5 - 10	10 – 14.5

Based on the environmental PCA, there are two groups of variables along the PC1 axis that represents high values of TPAH (identified as the presence of pollution), salinity, and

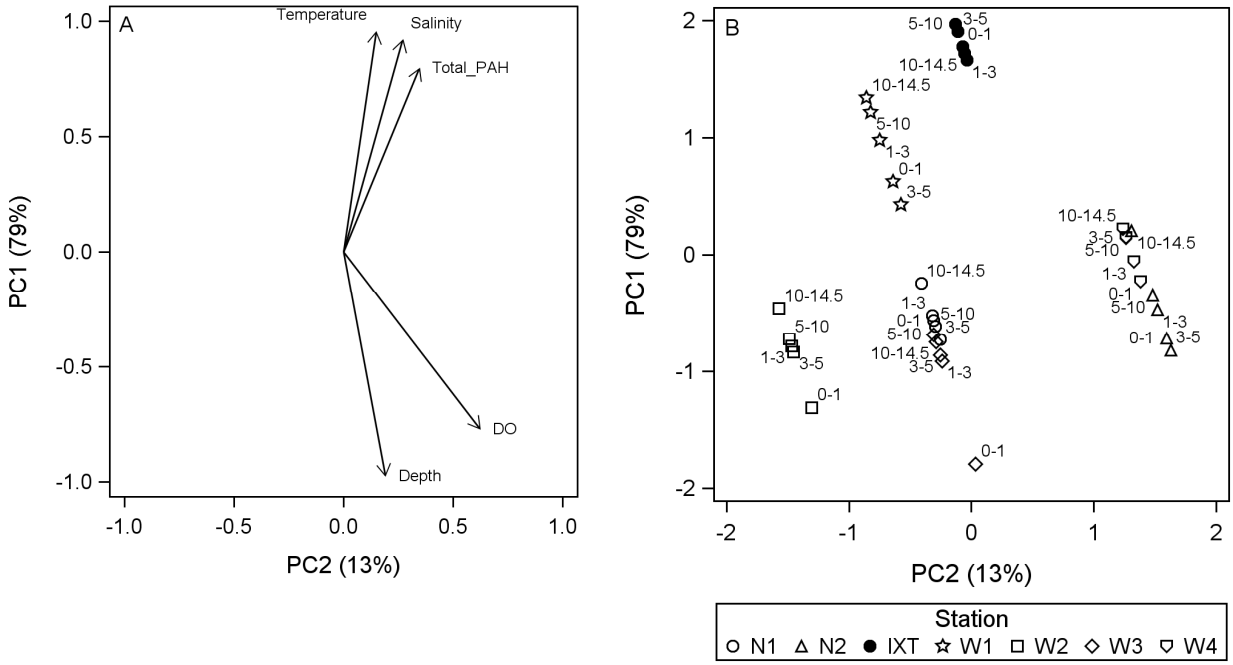

temperature (depth) as positive values, and low dissolved oxygen and deep depths as negative values (Fig. 2A). PC1 accounted for 68% and PC2 accounted for 20% of the variation. The combination of pollution and depth ocurrs because stations IXT and W1 had the highest TPAH concentrations but were also the shallowest and warmest waters (Fig. 2B). The vertical sections within stations group together, but stations are separate, meaning there is more similarity within sediment depths at a station than among the stations (Fig. 2B). Only the two furthest and deepest stations, N2 and W3, overlap and appear to be similar.

Fig. 2. Principal components analysis of the environmental variables measured at each station. A) Variable vector loads. B) Sample scores for sediment section depths at stations.

3.1.2 Macrofauna

Macrofauna and meiofauna community metrics were compared in the top 3 cm of sediment (Table 4). The highest macrofauna average abundance was at IXT (60 m), as much as

8.8 times higher, which also had the lowest diversity, as much as 1.9 times lower. The lowest macrofauna richness was at N2 (1240 m), as much as 1.8 times lower.

Table 4. Two-way partially heirarchical ANOVA results for macrofauna square root total abundance, Hill's N1 diversity, and richness across stations and section. A) ANOVA table. B) Tukey HSD test results for abundance by station. C) Tukey HSD test results for abundance by section. D) Tukey HSD test for diversity by section. E) Tukey HSD test results for richness by section.

A)		Abundance		Diversity		Richness	
Source	DF	F Value	Pr > F	F Value	Pr > F	F Value	Pr > F
Station	6	10.26	0.0004	1.42	0.2333	2.61	0.0745
Replicate(Station)	12	1.13	0.3708	0.98	0.4845	0.72	0.7260
Section	3	15.06	<0.0001	6.52	0.0012	15.60	<0.0001
Station*Section	18	1.34	0.2201	0.88	0.6064	0.68	0.8029

B)				Abundance			
Mean	83.5	55.2	52.2	44.1	39.1	38.1	33.9
Station	IXT	W1	W1	N1	W2	N2	W3

C)		Abundance		
Mean	66.4	59.4	37.9	35.9
Section	0 - 1	1 - 3	5 - 10	3 - 5

D)		Diversity		
Mean	4.53	3.66	2.82	2.7
Section	0 - 1	1 - 3	5 - 10	3 - 5

E)		Richness		
Mean	7.16	5.53	3.63	3.16
Section	0 - 1	1 - 3	5 - 10	3 - 5

The nMDS and CLUSTER analysis for macrofauna across all sediment sections found IXT (60 m) was different from all other stations at 52% similarity (Fig. 3). The one-way ANOSIM across stations confirmed a difference between stations (R=0.664, P = 0.001, n = 19). The one-way SIMPER analysis found that the differences between stations was attributed to 6 different taxonomic groups the isopod *Asellota*, polychaetes, oligochaetes, nematodes,

amphipods, and tanaids. There was not one group that dominated the differences between all stations.

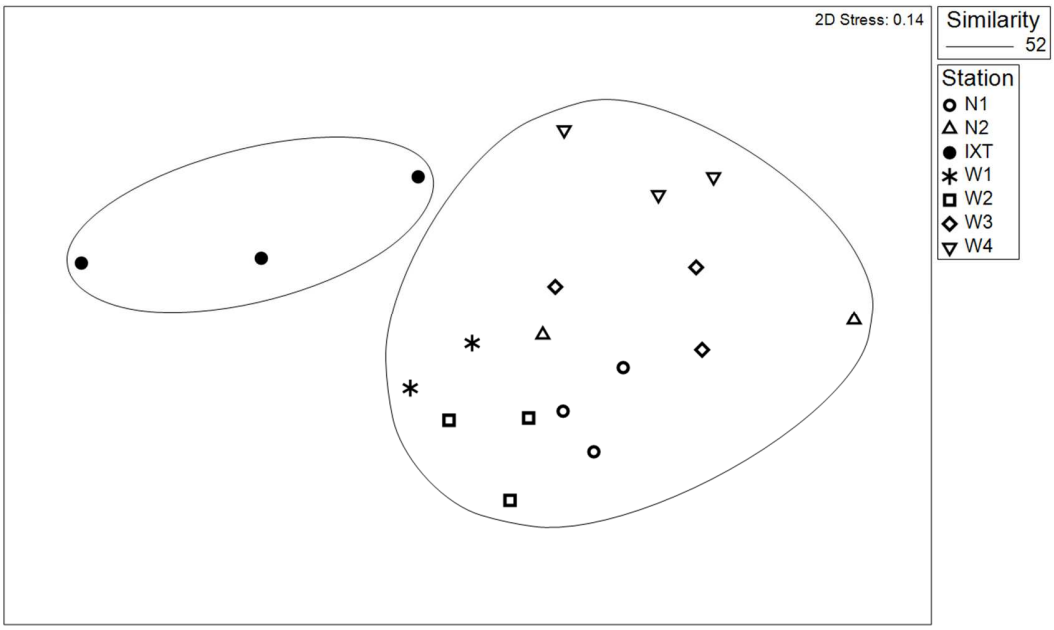

Fig. 3. A nMDS plot of differences among replicates within stations based on the macrofauna community structure integrated by sediment depth. The lines represent samples that share the same percent similarity.

3.1.3 Meiofauna

Meiofauna average abundance and diversity was highest at IXT (60 m), as much as 3.2 and 1.3 times higher respectively, while richness was highest at W1 (179 m), as much as 2 times higher (Table 5). The lowest diversity and richness was at W3 (1440 m). Total abundance (square root transformed) differed by station ($F_{6,24}$ = 5.36, P = 0.0067) and section ($F_{1,24}$ = 12.53, P = 0.0041). Abundance in IXT was up to 3.2 times higher than W1, N2, W1, W3 and W2.

Table 5. Two-way partially heirarchical ANOVA results for meiofauna square root total abundance, Hill's N1 diversity, and richness across stations and section. A) ANOVA table.

B) Tukey HSD test results for abundance by station. C) Tukey HSD test results for richness by station. D) Tukey HSD test results for diversity by station. E) Tukey HSD test results for abundance by section. F) Tukey HSD test results for diversity by section. G) Tukey HSD test results for richness by section.

A)		Abundance		Diversity		Richness	
Source	DF	F Value	Pr > F	F Value	Pr > F	F Value	Pr > F
Station	6	5.36	0.0067	3.12	0.0441	3.31	0.0369
Replicate(Station)	12	2.26	0.0857	1.05	0.4681	3.68	0.0161
Section	1	12.53	0.0041	150.19	<0.0001	114.51	<0.0001
Station*Section	6	1.45	0.2731	4.84	0.0099	3.26	0.0386

B)	Abundance						
Mean	761,000	528,000	291,000	272,000	264,000	240,000	238,000
Station	IXT	N1	W1	N2	W1	W3	W2

C)	Richness						
Mean	27	23.7	18.8	17.8	17.3	16.7	13.8
Station	W1	IXT	N1	W2	N2	W1	W3

D)	Diversity						
Mean	2.93	2.69	2.43	2.41	2.30	2.27	2.23
Station	IXT	W2	W1	N1	W1	N2	W3

E)	Abundance	
Mean	640	536
Section	0 - 1	1 - 3

F)	Diversity	
Mean	3.18	1.79
Section	0 - 1	1 - 3

G)	Richness	
Mean	23.8	14.2
Section	0 - 1	1 - 3

The nMDS and CLUSTER analysis for meiofauna in the top 3 cm found that IXT was different from all other stations except N1 replicate 2 at 60.83% similarity (Fig. 4). Stations W1

was different from stations N1, N2, W1, W2, and W3 at 72.48% (Fig. 4). The one-way ANOSIM across stations confirmed a significant difference between stations (R = 0.569, P-value = 0.001, n = 19). The one-way SIMPER analysis found that nematodes were the taxonomic group contributing the most to differences between stations, with nematodes contributing up to 25.73% of the dissimilarity and the highest abundances at IXT. For 6 of the 21 comparisons the highest contributing groups were either nauplii or gastrotrichs.

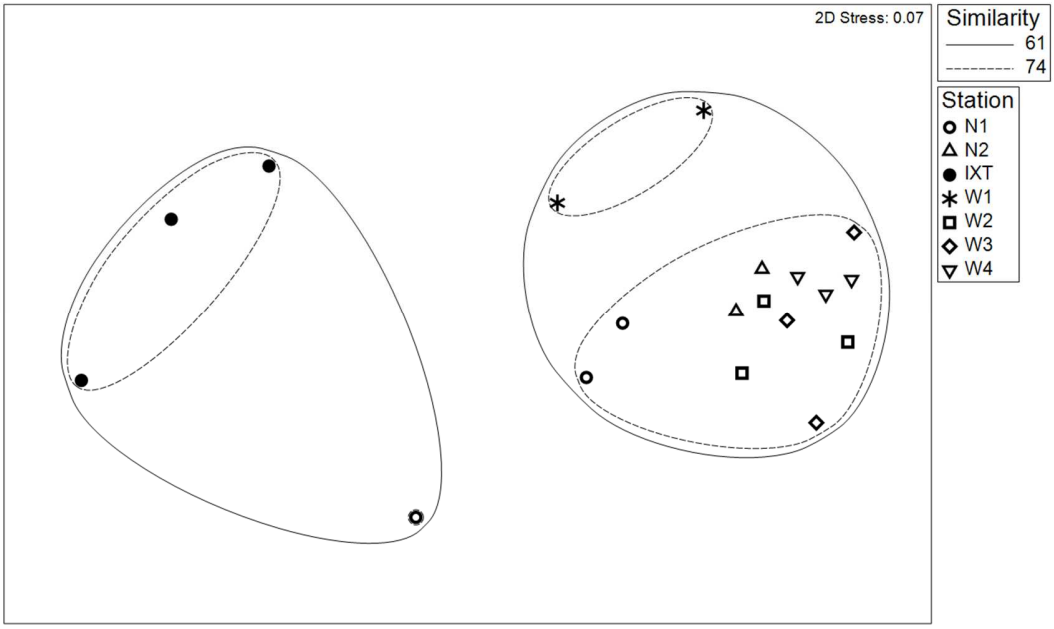

Fig. 4. A nMDS plot differences among replicates within stations based on the meiofauna community integrated by sediment depth. The lines represent samples that share the same percent similarity.

3.2 Sediment depth trends

3.2.1 PAH

Even though the station*section interaction was not significant (Table 3), the section with the highest concentration varied by station, with the highest (up to 6.3 times higher) found from 3 – 5 cm at station W1 (Fig. 5).

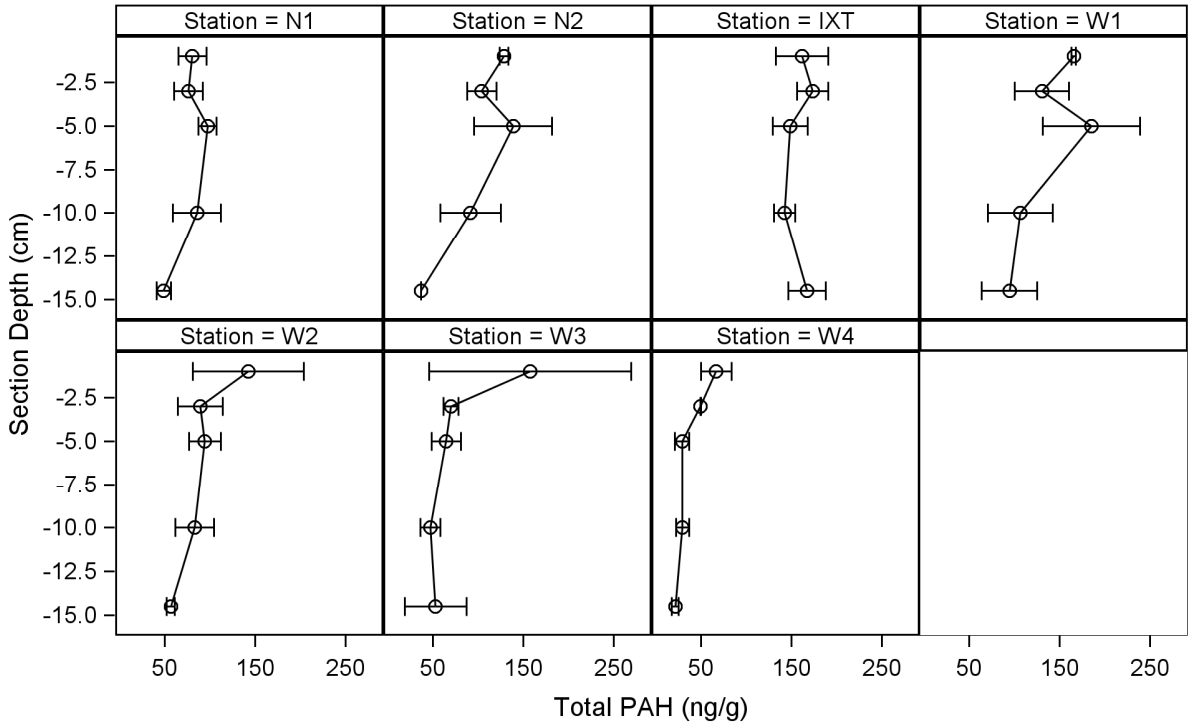

Fig. 5. Total PAH concentration across stations by sediment core sections. Boxes indicate the location of highest concentrations at each station.

3.2.2 Macrofauna

Average total macrofauna abundance (square root transformed) differed by station ($F_{6,12}$ = 10.26, P = 0.0004) and section ($F_{3,36}$ = 15.06, P = <0.0001) (Table 5). With the abundance at IXTOC1 being higher (up to 2.5 times higher) than all others (Fig. 6 and Table 5). Abundance in section 0 – 1 cm was higher (up to 1.8 times higher) than sections 3 – 5 and 5 – 10 cm (Fig. 6 and Table 5).

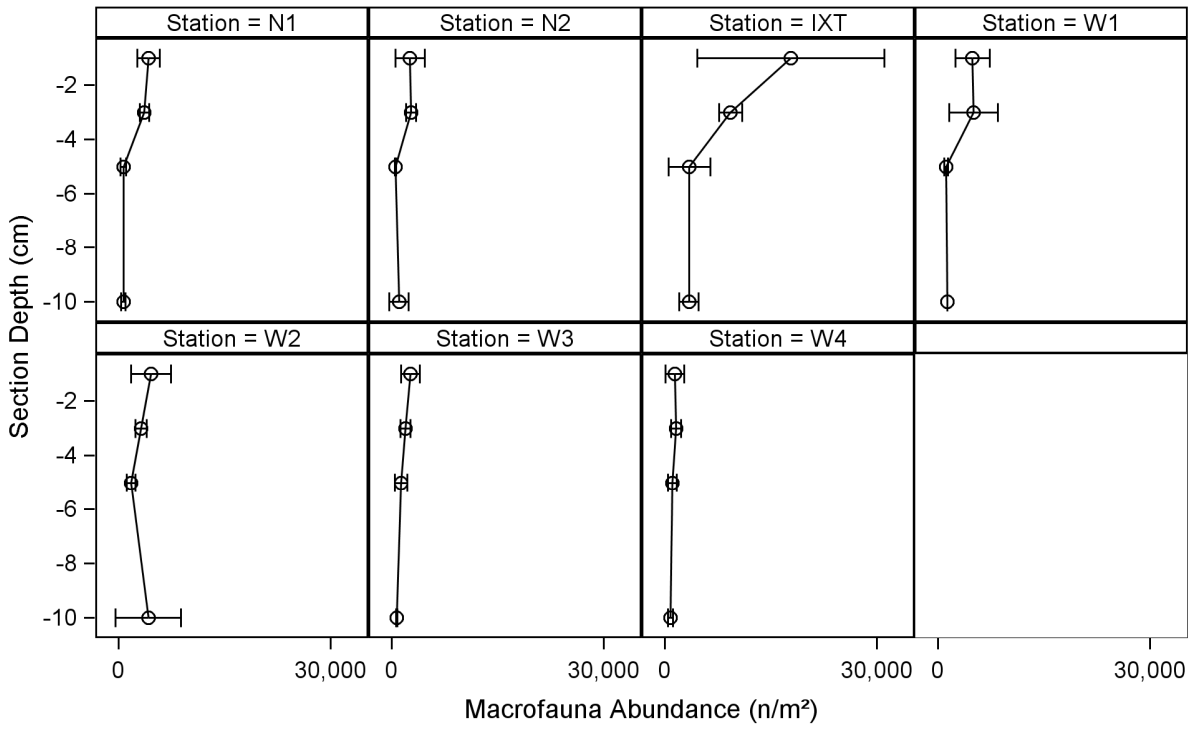

338

339 Fig. 6. Total untransformed macrofauna average abundance across stations by sediment core
340 sections.
341

342 Hill's N1 diversity and richness was different by section only ($F_{3,48}$ = 6.52, P = 0.0012
343 and $F_{3,48}$ = 15.60, P= <0.0001 respectively) (Table 5). Diversity was up to 1.7 times higher in
344 section 0 – 1 cm than sections 3 – 5 and 5 – 10 cm (Table 5). Richness was higher (up to 2.3
345 times higher respectively) in the top two sections 0 – 1 and 1 – 3 cm compared to the bottom two
346 (Fig. 7).

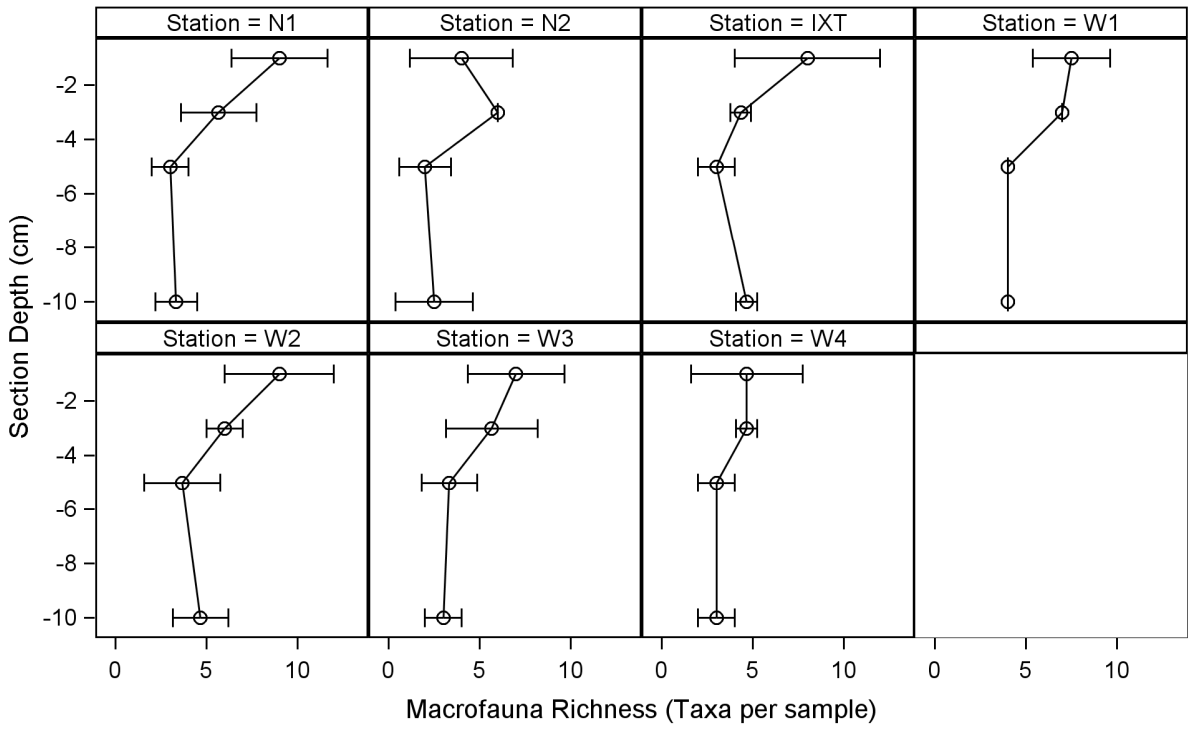

Fig. 7. Macrofauna taxa richness across stations by sediment core sections.

At stations N1, N2, and W1 section 3 – 5 cm when abundance, diversity, and richness was lowest TPAH concentrations were highest (Figs. 6 – 7).

3.2.3 Meiofauna

Total abundance (square root transformed) differed by station ($F_{6,12}$ = 5.36, P = 0.0067) and section ($F_{1,12}$ = 12.53, P = 0.0041) (Table 5). Section 0 – 1 cm was significantly 1.2 times higher than the 1 – 3 cm section (Fig.8). For Hill's N1 diversity station ($F_{6,12}$ = 3.12, P = 0.0441), section ($F_{1,12}$ = 150.19, P = <0.0001), and the station*section interaction ($F_{6,124}$ = 4.84, P = 0.0099) was significant (Table 5). Richness differed by station ($F_{6,12}$ = 3.31, P = 0.0369) and section ($F_{1,12}$ = 114.51, P = <0.0001) (Table 5). W1 had a higher richness (up to 2 times higher) than W2, N2, W1, and W3 (Fig. 9). Richness was highest in the top 1 cm (up to 1.7 times

higher) (Fig. 9). Nematode abundance was significantly different by station ($F_{6,12}$ = 5.04, P = 0.0084) (Table 6). Nematode abundance was higher (up to 3.4 times higher) at IXT than W1, N2, W1, W3, and W2 (Table 6). Copepod abundance differed by section ($F_{1, 12}$ = 117.8, P = <0.0001) with a significant station*section interaction (F = 3.85, P = 0.0224). Copepod abundance was higher (up to 3.8 times higher) in the 0 – 1 cm section (Table 6). The NC ratio was different by station ($F_{6, 12}$ = 16.15, P = <0.0001), section ($F_{1, 12}$ = 115, P = <0.0001), and the station*section interaction was significant ($F_{6,12}$ = 8.22, P = 0.0011) (Table 6 and Fig. 10). The interaction occurred because of an increased difference in NC between sections at IXT (8.9 times higher in 1 – 3 cm) and a decreased difference in sections at station W2 (0.98 times higher in 1 – 3 cm). For all but station IXT richness was high when TPAH was high.

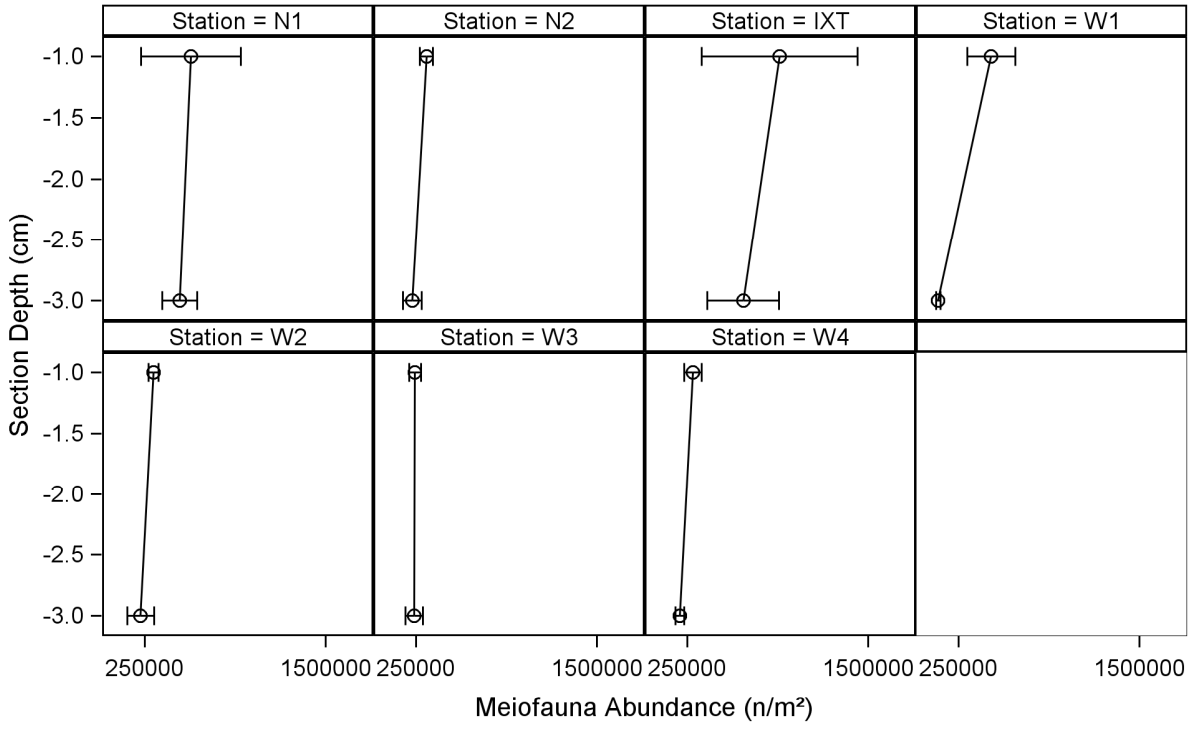

Fig. 8. Average total meiofauna abundance across stations by sediment core sections. Stations are in order of orientation and distance from wellhead.

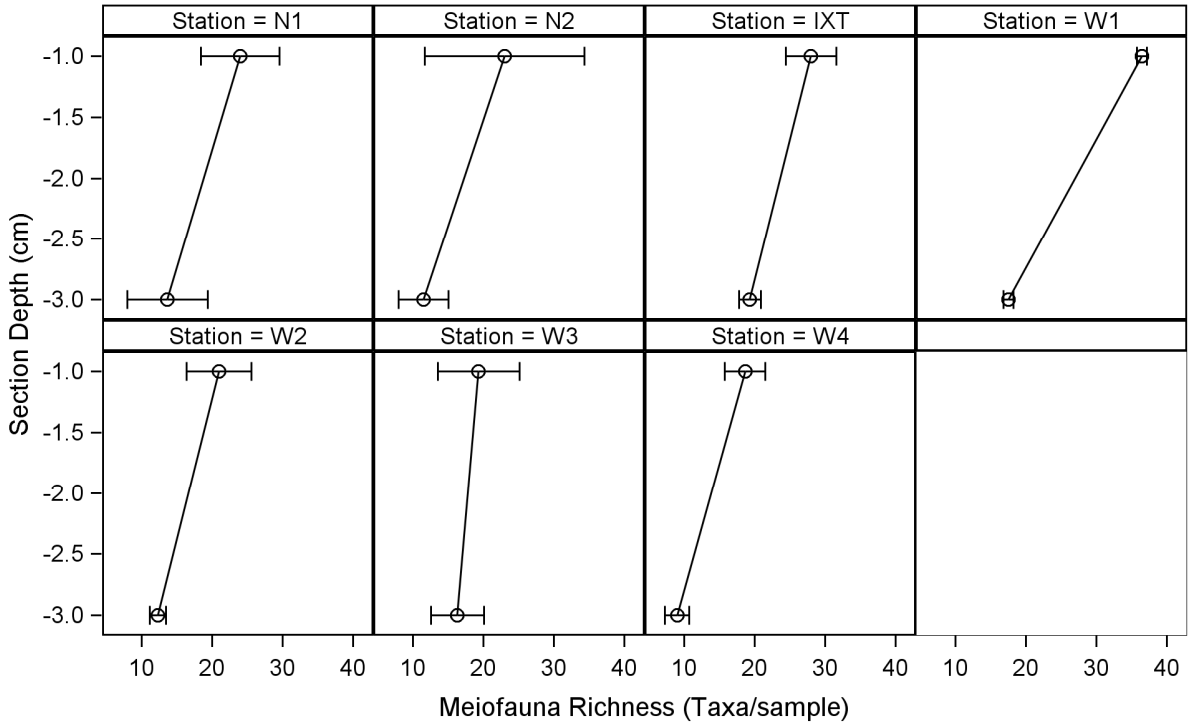

Fig. 9. Average meiofauna richness across stations by sediment core sections. Stations are in order of orientation and distance from wellhead.

Table 6. Two-way partially heirarchial ANOVA results for nematode abundance, copepod abundance, and the nematode copepod ratio (NC). All square root transformed.

A)		Nematode		Copepod		NC	
Source	DF	F Value	Pr > F	F Value	Pr > F	F Value	Pr > F
Station	6	5.04	0.0084	3.24	0.0394	16.15	<0.0001
Replicate(Station)	12	2.26	0.0861	1.11	0.4288	1.28	0.3397
Section	1	3.91	0.0715	117.80	<0.0001	115.00	<0.0001
Station*Section	6	1.46	0.2722	3.85	0.0224	8.22	0.0011
B)				Nematode			
Mean	657,000	454,000	247,000	229,000	208,000	204,000	193,000
Station	IXT	N1	W1	N2	W1	W3	W2
C)				NC			
Mean	36.5	17.7	16.8	9.42	8.57	8.36	5.61

Station	IXT	W1	N1	W3	W1	N2	W2
E)	Diversity						
Mean	3.18	1.79					
Section	0 – 1	1 – 3					
F)	Copepod						
Mean	62,400	16,300					
Section	0 – 1	1 – 3					
G)	NC						
Mean	23.8	6.00					
Section	1 – 3	0 – 1					

383

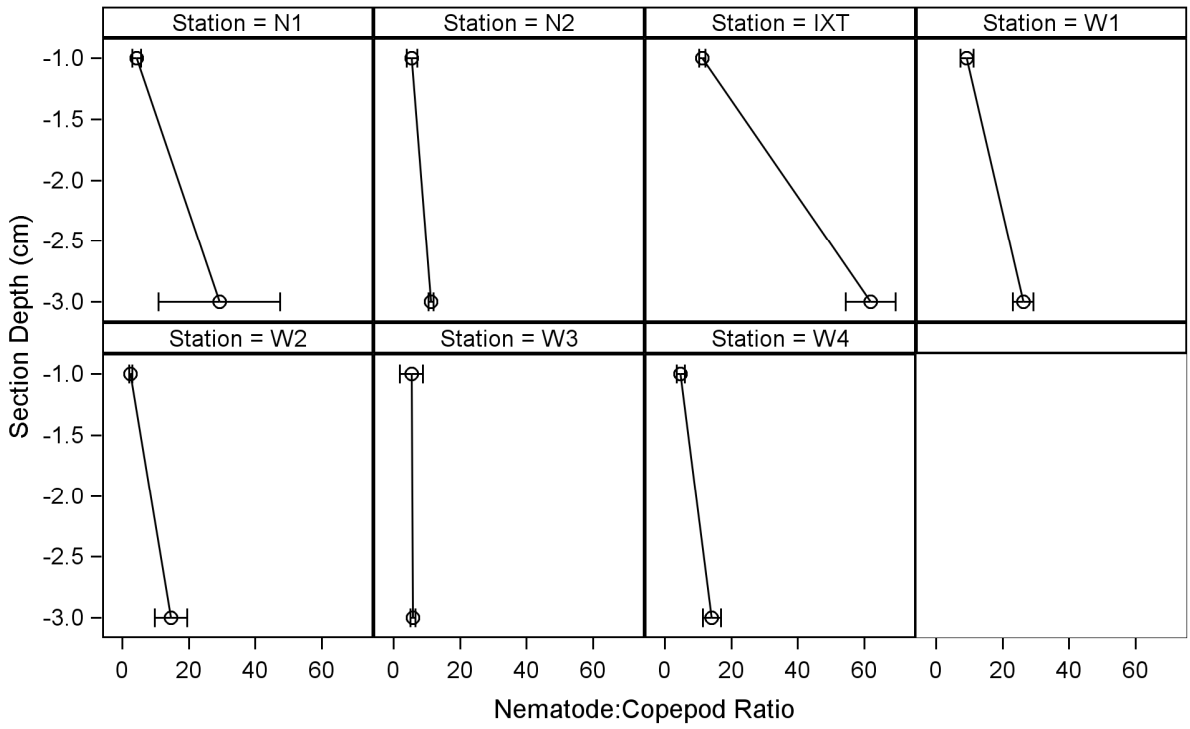

384

385 **Fig. 10. Average nematode copepod ratio (NC) across stations by sediment depth sections.**
386 **Stations are in order of orientation and distance from wellhead.**

387

388 **4 Discussion**

389 The premise of this study is that the vertical distribution of sediments provides a
390 chronological record that reflects information about past events. It is assumed that the area
391 around the DWH wellhead will recover once the contaminated sediment is buried below the
392 biologically active zone of 10 cm based on vertical distributions of macrofauna and meiofauna in
393 studies of baseline sites (Montagna et al., 2017). The Ixtoc-1 spill, which occurred 36 years prior
394 to the current sampling, provides a test case for determining if the chronology premise is correct,
395 so the approach could be used to estimate the recovery rate of the DWH impact area. However,
396 an important assumption of this study is that the sediment remains vertically laminated so that
397 layers can be identified at depths that represent different time frames. Finally, chemical and

biological data must be considered together because as the assessment is to determine if biological metrics are changing in response to chemical metrics.

There is an important difference between the two spills, because the DWH affected benthos are in the deep sea, but the Ixtoc affected benthos span great depth ranges. The Ixtoc plume moved to the west, and therefore moved over great depth ranges (Sun et al. 2015). So, whereas the DWH depths remain deep-sea in nature, the Ixtoc depths range from shallow to deep. The sampling stations (Table 1) were chosen based on the results provided by Sun et al. (2015). Depth is thus a confounding factor in the current study, because benthic community structure is known to change with depth. Additionally, it is possible that shallow areas would have sediments that are vertically mixed by waves or currents.

Of the seven stations sampled, W1 and IXT were classified as having the shallowest water depth (179 and 60 m respectively), highest temperature, highest salinity, and highest TPAH concentration compared to the other stations (Table 2 and Fig. 2B). Therefore, TPAH concentration is correlated with all these variables (inversely by water depth, and positively with temperature and salinity) along PC1 (Fig. 2A). However, it is interesting that IXT has the highest TPAH concentration (Tables 2 and 3) because this may be a remnant of the Ixtoc-1 oil spill, or continuous seeping from nearby seeps, or continued petroleum production activity in the area. The IXT station is closest to the original wellhead location, but the trend observed in the mixed sediments indicates PAHs main source might be from petroleum production activity. The Campeche Bay area is still an active petroleum production area and W1 and IXT are closest to the ongoing oil and gas production (Fig. 11), which would confound any Ixtoc-1 chemical signals and biological effects. However, the highest concentrations of TPAHs were found in the 3 – 5 cm and 1 – 3 cm sections respectively and not on the surface (Fig. 5). The elevated levels

421 at these sediment depths below the surface could be from the Ixtoc-1 oil spill because a signal
422 was found from 2.4 – 2.8 cm depth at two other stations, which is close to the depths of elevated
423 TPAH levels (Table 2, Fig. 5).

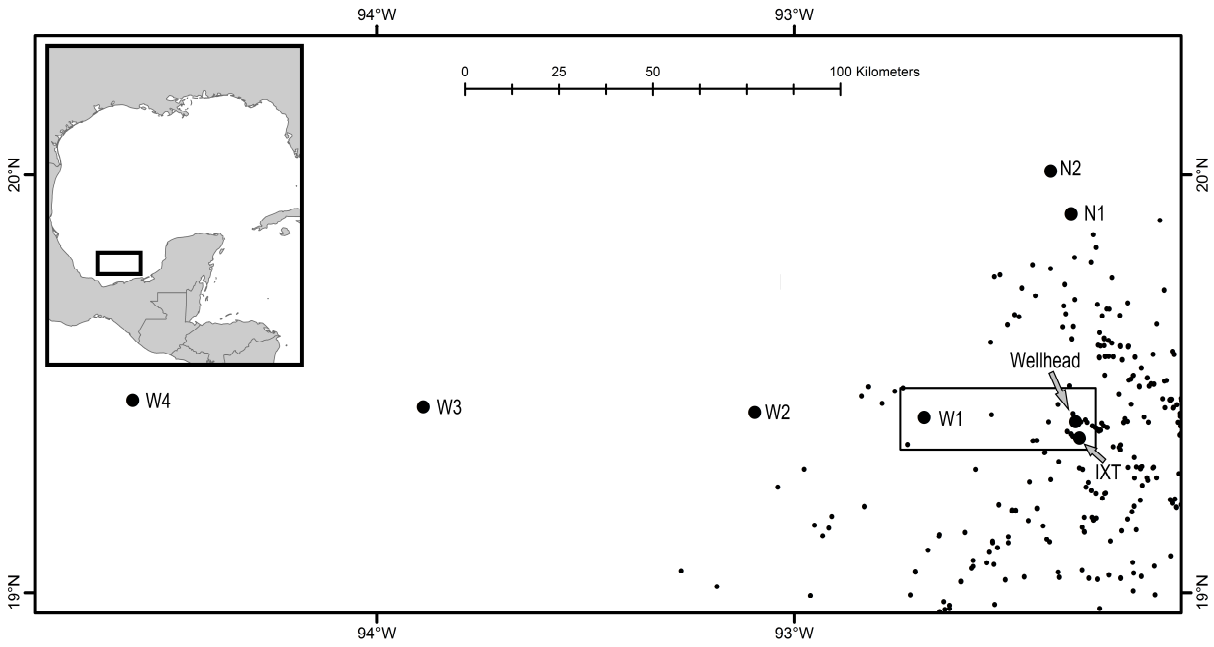

424

425 **Fig. 11. Map showing the location of the sample stations (large circles, station names in**
426 **Fig. 1) and shallow wells (small circles). Box = W1, IXT, and Ixtoc-1 wellhead.**
427

428 The TPAH concentrations in the area are low compared to other regions and sediment
429 quality standards. The highest TPAH concentration of 173 ppb, at station IXT 1-3 cm, was not
430 far above the median value of 92 ppb for background TPAH concentrations in the northern Gulf
431 of Mexico (Wade et al., 2008). The Ixtoc-1 area TPAH values are below the sediment quality
432 minimum effects range developed for nearshore benthic fauna of 4022 ppb (Long et al., 1995).
433 However, it can't be assumed that shallow water animals have the same sensitivity as deeper
434 living animals. Shallow water environments, like the coastal areas of the Gulf of Mexico, have
435 an order of magnitude higher PAH concentrations than offshore continental shelf sediments

436 (Kennicutt et al., 1996). Field observations following the DWH found moderate benthic effects
437 (i.e., a 5% loss of macrofauna diversity and a 19% loss of meiofauna diversity) starting at 370
438 ppb (Montagna et al., 2013; Baguley et al., 2015). The average PAH value in the DWH
439 impacted zones where benthic community effects are still being observed after four years was
440 218 ppb (Reuscher et al., 2017). Estuarine organisms that are always exposed to higher
441 concentrations could be more tolerant of PAH than offshore organisms. In addition, the animals
442 around the Ixtoc oil spill site have been undergoing chronic exposure. The sediment quality
443 standards proposed by Long et al. (1995) are all based on acute exposure. None of the studies
444 reviewed ran for longer than 4 months (Long et al., 1995), the Ixtoc oil spill occurred over 30
445 years ago. Therefore, even though the PAH levels are lower, it does not mean there is no toxic
446 effect. Hydrocarbon exploration and production has occurred for many infauna generations at the
447 Ixtoc site, so it is possible that organisms in this area can tolerate existing levels of PAH.

448 The macrofauna community exhibits signs of disturbance, but not at all locations. Higher
449 abundance and low diversity were found at station IXT (Fig. 6, Table 4). This combination of
450 benthic metrics was also found in the severely and moderately impacted area around the DWH
451 wellhead (Montagna et al., 2013; Washburn et al., 2017; Washburn et al., 2018). Impacts were
452 classified as severe at locations within 3 km of the DWH wellhead, and as moderate within 15
453 km of the wellhead (Washburn et al. 2017). A 54% loss of macrofauna diversity and a 38% loss
454 of meiofauna diversity were classified as severe effects (Montagna et al., 2013). This same trend
455 was also seen four years after the spill when macrofauna where compared between impacted and
456 non-impacted locations (Reuscher et al. 2017). Contaminant presence is also evident by
457 sediment depth (Table 4). Overall, macrofauna abundance, diversity, and richness were highest
458 in the top 3 cm. This is the typical vertical pattern because the superficial sediments have greater

459 dissolved oxygen concentrations and food availability, particularly in the deep sea as in
460 shallower depth zones (Giere, 2009; Montagna et al., 2017). When macrofauna community
461 metrics by sediment depth were compared to PAH concentrations in this study, both potential
462 toxic effects and enrichment effects were identified. A toxic effect is expected to cause a
463 decrease in the abundance and diversity of the organisms (Jacobs, 1980; Sanders et al., 1980).
464 At stations N1, N2 and W1 high PAH concentration corresponded to low abundance, richness,
465 and diversity values at 3 – 5 cm sediment depth (Figs. 6 – 7). At station IXT the high PAH
466 concentration corresponded to low diversity (Figs. 6 – 7), but not to low abundance and richness.
467 Therefore, the macrofauna at station IXT are likely experiencing a moderate level of disturbance,
468 which is likely due to both the Ixtoc spill and the legacy of pollution at the site.

469 For meiofauna the highest abundance and diversity were found at station IXT (Fig. 8, and
470 Table 5). Organic enrichment is expected to result in high abundances of opportunistic and/or
471 tolerant species, and thus low diversity in a contaminated area (Spies et al., 1988; Jewett et al.,
472 1999; Washburn et al., 2017). However, at IXT there is both high abundance and high diversity.
473 Increased meiofauna abundance and diversity was also observed in the presence of marine snow
474 and petroleum during a microcosm experiment (Rohal et al., 2020). A similar increase in
475 nematode abundance was found near petroleum platforms, which was attributed to increased
476 food availability due to presence of fouling communities on platforms (Montagna and Harper,
477 1996). A higher Nematode to Copepod (NC) ratio is believed to be indicative of chemically and
478 organically polluted locations, near seeps, sewage outfalls, and in low dissolved oxygen areas
479 (Raffaelli and Mason, 1981; Shirayama and Ohta, 1990; Sellanes et al., 2010). The highest NC
480 ratio was found at IXT (Table 6; Fig. 10), which could be indicating organic matter enrichment
481 at this location. It must be noted that the IXT site is the shallowest, is nearest to land, and is in

482 the midst of many other platforms, so the high NC could be due to one or more of all these
483 drivers. Also, the NC ratio was the only benthic metric that correlated with PC1 (Table S1),
484 which indicates that the NC ratio is high when the salinity, temperature, and TPAH concentration
485 is high.

486 Overall, meiofauna abundance, diversity, and richness were highest in the top 1 cm as is
487 expected (Table 5). However, significant station*section interactions occurred for nearly all
488 meiofauna metrics including meiofauna diversity, meiofauna richness, copepod abundance, NC
489 ratio, which indicates different processes are occurring at each station. This is likely attributed to
490 ongoing changes in the surficial sediment influenced by ongoing petroleum production activity,
491 and station depth. The NC ratio was much higher at station IXT in the 1 – 3 cm section
492 compared to all other stations. High NC ratio values could be indications of chemical pollution
493 because it was one of the key indicators of the DWH oil spill (Montagna et al., 2013, Baguley et
494 al. 2015).

495 An Ixtoc-1 biogeochemical signal from foraminiferan isotopic data was found at stations
496 W1 and W3 between 2.4 – 2.8 cm sediment depths (Table 2). This burial of the Ixtoc-1
497 chemicals does not mean that recovery has occurred for three reasons. First, sampling over a
498 large spatial scale is key to assessing impacts so that the event is not indistinguishable from
499 natural variability. Only seven stations were included in the current analysis therefore, it is
500 likely that power to detect change caused by the Ixtoc-1 spill is low in the current study. Second,
501 no Ixtoc-1 biogeochemical signal from foraminiferan isotopic data was detected at the two
502 stations closest to the wellhead because the surface sediment appeared to be mixed and no
503 evidence of lamination was found in the cores collected at those stations. But, TPAH
504 concentration was highest at the 1 – 3 cm section at station IXT where an Ixtoc-1 signal would

505 be expected based on sedimentation rates. Macrofauna diversity was lowest at the 1 – 3 cm
506 section, which is unusual because the trend is for diversity/richness to decrease as depth in the
507 sediment increases (Montagna et al., 2017). The NC ratio was much higher at station IXT in the
508 1 – 3 cm section compared to all other stations. High NC ratio values are indications of chemical
509 pollution, low dissolved oxygen concentrations, and seepage and were one of the key indicators
510 of the DWH oil spill (Montagna et al., 2013). TPAH concentration, macrofauna diversity with
511 depth, and NC ratio with depth at station IXT suggest that recovery has not occurred after more
512 than 30 years. Third, individual sediment depth profiles for each station indicate that different
513 processes are happening at each location that can be related to the depth zone. The ongoing
514 petroleum activity in the area has likely impacted each station to varying degrees and could be
515 masking any residual Ixtoc-1 affects. At stations W1 and W3, where an Ixtoc-1 signal was found
516 within the 1– 3 cm section there is a larger NC ratio when compared to station W2 which is at a
517 comparable depth and had no Ixtoc-1 signal. Even though the number of copepods naturally
518 decreases with sediment depth the differences between stations should be consistent across
519 similar depths. The NC ratio high values at these stations likely indicates a continued Ixtoc-1
520 response based on observational evidence despite the lack of statistical validation.

521 In conclusion, the benthic community metrics around the site of the Ixtoc-1 oil spill
522 supports the interpretation that recovery is in progress. The assumption is that recovery will
523 occur when the contaminated sediment moves below the biologically active zone. Based on
524 measurements made by Schwing and Machain-Castillo (2020, Table 2), an average Ixtoc-1
525 signal depth of 2.6 cm after 36 years yields a sedimentation rate is about 0.072 cm/year (range
526 from 0.067 – 0.078). At the rate, it will take about 103 (range from 92 - 113) more years beyond
527 2015 until the benthic community has completely displaced the polluted sediment at more than

10 cm depth being then recovered from the Ixtoc-1 oil spill. The total will be 139 (range 128 – 149) years for recovery to occur. However, sedimentation rate is variable in space and time and the same rate will not apply to the area near the DWH wellhead. Sedimentation rates nearest the DWH wellhead, although deeper, range from 0.1 – 0.3 cm/year naturally with higher rates after the spill (Brooks et al., 2015) because of the closeness to the continental break and the occurrence on the continental slope and Mississippi fan. Based on an average rate of 0.2 cm/year the benthic community around the DWH well head will recover 50 (range 33 to 100) years after the well was capped.

Acknowledgments

Research was partially supported by a grant from The Gulf of Mexico Research Initiative/C-IMAGE II, No. SA 15-16. Data are publicly available through the Gulf of Mexico Research Initiative Information & Data Cooperative (GRIIDC) at https://data.gulfresearchinitiative.org (doi: R4.x267.000:0116). This publication was made partially possible by the National Oceanic and Atmospheric Administration, Office of Education Educational Partnership Program award (NA16SEC4810009). Its contents are solely the responsibility of the award recipient and do not necessarily represent the official views of the U.S. Department of Commerce, National Oceanic and Atmospheric Administration. Research was also partially supported by a Harte Research Fellowship provided by the Harte Research Institute at Texas A&M University-Corpus Christi (TAMUCC). Many people at TAMUCC helped in completing this project. Elani Morgan (TAMUCC) helped with data management. Tiffany Hawkins, Courtney Armstrong, and Meagan Hardegree helped with sorting of the samples. Larry Hyde and Michael Reuscher helped with animal identification. Dr. Lee Smee and Dr. Jeff Baguley helped critique the manuscript.

553 **References**

554 Adhikari, P.L., Wong, R.L., Overton, E.B., 2017. Application of enhanced gas
555 chromatography/triple quadrupole mass spectrometry for monitoring petroleum
556 weathering and forensic source fingerprinting in samples impacted by the Deepwater
557 Horizon oil spill. Chemosphere 184, 939–950.
558 https://doi.org/10.1016/j.chemosphere.2017.06.077.
559 Baguley, J.G., Montagna, P.A., Cooksey, C., Hyland, J.L., Bang, H.W., Morrison, C.,
560 Kamikawa, A., Bennetts, P., Saiyo, G., Parsons, E., Herdener, M., Ricci, M., 2015.
561 Community response of the deep-sea soft-sediment metazoan meiofauna to the
562 Deepwater Horizon blowout and oil spill. Mar. Ecol. Prog. Ser. 528, 127-140.
563 https://doi.org/10.2254/meps11290.
564 Beriro, D.J., Vane, C.H., Cave, M.R., Nathanail, C.P., 2014. Effects of drying and comminution
565 type on the quantification of Polycyclic Aromatic Hydrocarbons (PAH) in a homogenised
566 gasworks soil and the implications for human health risk assessment. Chemosphere 111,
567 396-404. https://doi.org/10.1016/j.chemosphere.2014.03.077.
568 Brooks, G.R., Larson, R.A., Schwing, P.T., Romero, I., Moore, C., Reichart, G.J., Jilbert, T.,
569 Chanton, J.P., Hastings, D.W., Overholt, W.A., Marks, K.P., Kostka, J.E., Holmes, C.Q.,
570 Hollander, D., 2015. Sedimentation pulse in the NE Gulf of Mexico following the 2010
571 DWH blowout. PLoS ONE: 10(7): e0132341.
572 https://doi.org/10.1371/journal.pone.0132341.
573 Carlisle, K.M., 2014. The Large Marine Ecosystem approach: Application of an integrated,
574 modular strategy in projects supported by the Global Environment Facility. Environ.
575 Develop. 11, 19-42. https://doi.org/10.1016/j.envdev.2013.10.003.

576 Daly, K., Passow, U., Chanton, J., Hollander, D., 2016. Assessing the impacts of oil-associated
577 marine snow formation and sedimentation during and after the Deepwater Horizon oil
578 spill. Anthropocene, 13, 18-33. http://doi.org/10.1016/j.ancene.2016.01.006
579 Danovaro, R. 2010. Methods for the Study of Deep-Sea Sediments, Their Functioning and
580 Biodiversity, CRC Press, Boca Raton, Florida, USA.
581 DWH Natural Resource Trustees, 2016. Deepwater Horizon oil spill: Final programmatic
582 damage assessment and restoration plan and final programmatic environmental impact
583 statement. [cited 2016 April 5]. Available from:
584 http://www.gulfspillrestoration.noaa.gov/wp-content/uploads/Chapter-2_Incident-
585 Overview_508.pdf.
586 Giere, O., 2009. Meiobenthology the microscopic motile fauna of aquatic sediments, second ed.
587 Springer-Verlag, Berlin.
588 Jernelöv, A., Lindén, O., 1981. A cast study of the World's largest oil spill. Ambio 10, 299-306.
589 https://www.jstor.org/stable/4312725
590 Jernelöv, A. 2010. The threats from oil spills: now, then, and in the future. Ambio 39, 353-366.
591 https://doi.org/10.1007/s13280-010-0085-5.
592 Kennicutt, M.C., II, Green, R.H., Montagna, P., Roscigno, P.F., 1996. Gulf of Mexico Offshore
593 Operations Experiment (GOOMEX) Phase I: Sublethal responses to contaminant
594 exposure - introduction and overview. Can. J. Fish. Aquat. Sci. 53:2540-2553.
595 http://dx.doi.org/10.1139/cjfas-53-11-2540.
596 Long, E.R., Macdonald, D.D., Smith, S.L., Calder, F.D., Bin, C., Smith, S.L., 1995. Incidence of
597 adverse biological effects within ranges of chemical concentrations in marine and
598 estuarine sediments. Environ. Manage. 19, 81–97. https://doi.org/10.1007/BF02472006.

599 Jacobs, R.P.W.M., 1980. Effects of the 'Amoco Cadiz' oil spill on the seagrass community at
600 Roscoff with special reference to the benthic infauna. Mar. Ecol. Prog. Ser. 2, 207-212.
601 https://www.int-res.com/articles/meps/2/m002p207.pdf
602 Jewett, S.C., Dean, T.A., Smith, R.O., Blanchard. A., 1999. 'Exxon Valdez' oil spill: impacts
603 and recovery in the soft-bottom benthic community in and adjacent to eelgrass beds.
604 Mar. Ecol. Prog. Ser. 185, 59-83. https://doi.org/10.3354/meps185059.
605 Montagna, P.A, Baguley, J.G., Cooksey, C., Hartwell, I., Hyde, L.J., Hyland, J.L., Kalke, R.D.,
606 Kracker, L.M., Reuscher, M., Rhodes, A.C.E., 2013. Deep-Sea Benthic Footprint of the
607 Deepwater Horizon Blowout. PLoS ONE 8(8), e70540.
608 http://dx.doi.org/10.1371/journal.pone.0070540.
609 Montagna, P.A., Baguley, J.G., Hsiang, C.Y., Reuscher, M.G., 2017. Comparisons of sampling
610 methods for deep-sea infauna. Limnol. Oceanog. Meth. 15(2), 166-183.
611 http://dx.doi.org/10.1002/ieam.1791.
612 Oil Spill Intelligence Report. 1980. Volume III, Center for Short-Lived Phenomena, Cambridge,
613 MA.
614 Passow, U. 2016. Formation of rapidly-sinking, oil-associated marine snow. Deep-Sea Res. II
615 129, 232-240. https://doi.org/10.1016/j.dsr2.2014.10.001.
616 Passow, U., Ziervogel, K., Asper, V., Diercks, A., 2012. Marine snow formation in the aftermath
617 of the Deepwater Horizon oil spill in the Gulf of Mexico. Env. Res. Lett. 7(3), 035301.
618 https://doi.org/10.1088/1748-9326/7/3/035301.
619 Raffaelli, D.G., Mason, C.F., 1981. Pollution monitoring with meiofauna, using the ratio of
620 nematodes to copepods. Mar. Poll. Bull. 12, 158 – 163. https://doi.org/10.1016/0025-
621 326X(81)90227-7.

622 Reuscher, M.G., Baguley, J.G., Conrad-Forrest, N., Cooksey, C., Hyland, J.L, Lewis, C.,
623 Montagna, P.A., Ricker, R.W., Rohal, M., Washburn, T., 2017. Temporal patterns of
624 Deepwater Horizon impacts on the benthic infauna of the northern Gulf of Mexico
625 continental slope. PLoS ONE 12(6), e0179923.
626 https://doi.org/10.1371/journalpone.0179923.
627 Rohal, M., Barrera, N., van Eenennaam, J.S., Foekema, E.M., Montagna, P.A., Murk, A.J.,
628 Pryor, M., Romero, I.C., 2020. The impact of experimental oil-contaminated marine
629 snow on meiofauna. Mar. Poll. Bull. 150, 110656.
630 https://doi.org/10.1016/j.marpolbul.2019.110656.
631 Romero, I.C., 2019. A high-throughput method (ASE-GC /MS/MS/MRM) for quantification of
632 multiple hydrocarbon compounds in marine environmental samples. Mar. Technol. Soc.
633 J. 52, 66-70. https://doi.org/10.4031/MTSJ.52.6.6.
634 Romero, I.C., Chanton, J.P., Roseheim, B.E., Radović, J.R., Schwing, P.T., Hollander, D.J.,
635 Larter, S.R., Oldenburg, T.B.P., 2020. Long-term preservation of oil spill events in
636 sediments: the case for the Deepwater Horizon oil spill in the northern Gulf of Mexico
637 (Chap. 17).). In: Murawski, S.A., Ainsworth, C., Gilbert, S., Hollander, D., Paris, C.B.,
638 Schlüter, M., Wetzel, D. (Eds.), Deep Oil Spills: Facts, Fate, Effects. Springer, Cham,
639 Switzerland, pp 285-300.
640 Romero, I.C., Schwing, P.T., Brooks, G.R., Larson, R.A., Hastings, D.W., Flower, B.P.,
641 Goddard, E.A., Hollander, D.J., 2015. Hydrocarbons in deep sea sediments following the
642 2010 Deepwater Horizon Blowout in the Northeast Gulf of Mexico. PLoS ONE 10(5),
643 e0128371. https://doi.org/10.1371/journal.pone.0128371.

644 Romero, I.C., Sutton, T., Carr, B., Quintana-Rizzo E., Ross, S.W., Hollander. D.J., Torres, J.J.,
645 2018. Decadal assessment of polycyclic aromatic hydrocarbons in mesopelagic fishes
646 from the Gulf of Mexico reveals exposure to oil-derived sources. Environ. Sci. Technol.
647 52, 10985–10996. https://doi.org/10.1021/acs.est.8b02243.
648 Romero, I.C., Toro-Farmer, G., Diercks, A.R., Schwing, P.T., Muller-Karger, F., Murawski, S.,
649 Hollander, D.J., 2017. Large Scale deposition of weathered oil in the Gulf of Mexico
650 following a deepwater oil spill. Environ. Pollut. 228, 179-189.
651 http://dx.doi.org/10.1016/j.envpol.2017.05.019.
652 Ryerson, T.B., Camilli, R., Kessler, J.D., Kujawinski, E.B., Reddy C.M., 2012. Chemical data
653 quantify Deepwater Horizon hydrocarbon flow rate and environmental distribution. Proc.
654 Natl. Acad. Sci. 109, 20246-20253. www.pnas.org/cgi/doi/10.1073/pnas.1110564109.
655 Sanders, H.L, Grassle, J.F., Hampson, G.R., Morse, L.S., Garner-Price, S., Jones, C.C., 1980.
656 Anatomy of an oil spill: long-term effects from the grounding of the barge Florida off
657 west-Falmouth, Massachusetts. J. Mar. Res. 38, 265-380.
658 https://darchive.mblwhoilibrary.org/bitstream/handle/1912/3474/J%20marine%20researc
659 h%20v38%201980.pdf?sequence=1&isAllowed=y
660 SAS Institute Inc., 2017. SAS/STAT® 14.3 Users Guide. Cary, North Carolina, USA.
661 Schwing, P.T., Chanton, J.P., Romero, I.C., Hollander, D.J., Goddard, E.A., Brooks, G.R.,
662 Larson, R.A., 2018. Tracing the incorporation of carbon into benthic foraminiferal calcite
663 following the Deepwater Horizon event. Env. Poll. 237, 424-429.
664 Schwing, P.T., O'Malley, B.J., Romero, I.C., Martínez-Colón, M., Hastings, D.W., Glabach,
665 M.A., Hladky, E.M., Greco, A., Hollander, D.J., 2017a. Characterizing the variability of
666 benthic foraminifera in the northeastern Gulf of Mexico following the Deepwater

667 Horizon event (2010-2012). Env. Sci. Poll. Res. 24(3), 2754-2769.
668 https://doi.org/10.1007/s11356-016-7996-z.
669 Schwing, P.T., Brooks, G.R., Larson, R.A., O'Malley, B.J., Hollander, D.J., 2017b. Constraining
670 the spatial extent of the Marine Oil Snow Sedimentation and Accumulation (MOSSFA)
671 following the DWH event using a $^{210}Pb_{xs}$ inventory approach. Env. Sci. Tech. 51,
672 5962−5968. https://doi.org/10.1021/acs.est.7b00450.
673 Schwing P.T., Machain-Castillo, M.L., 2020a. Impact and resilience of benthic foraminifera in
674 the aftermath of the Deepwater Horizon and Ixtoc 1 oil spills (Chap. 23). In: Murawski,
675 S.A., Ainsworth, C., Gilbert, S., Hollander, D., Paris, C.B., Schlüter, M., Wetzel, D.
676 (Eds.), Deep Oil Spills: Facts, Fate, Effects. Springer, Cham, Switzerland, pp 374-387.
677 Schwing, P.T., Machain-Castillo, M.L., Brooks, G.R., Larson, R.A., Fillingham, J.N., Sanchez-
678 Cabeza, J.A., Ruiz-Fernández, A.C., Hollander, D.J., (In Prep). Multi-proxy assessment
679 of recent regional-scale events recorded in Southern Gulf of Mexico sediments.
680 Schwing, P.T., Montagna, P.A., Machain-Castillo, M.L., Escobar-Briones, E., Rohal, M., 2020b.
681 Benthic faunal baselines in the Gulf of Mexico: A precursor to evaluate future impacts
682 (Chap. 6). In: Murawski, S.A., Ainsworth, C., Gilbert, S., Hollander, D., Paris, C.B.,
683 Schlüter, M., Wetzel, D. (Eds.), Scenarios and Responses to Future Deep Oil Spills.
684 Springer, Cham, Switzerland, pp 96-108.
685 Sorensen, L., Meier, S., Mjos, S.A., 2016. Application of gas chromatography/tandem mass
686 spectrometry to determine a wide range of petrogenic alkylated polycyclic aromatic
687 hydrocarbons in biotic samples. Rapid Commun Mass Spectrom 30, 2052-2058.
688 https://doi.org/10.1002/rcm.7688.

689 Spies, R.B., Hardin, D.D., Toal, J.P., 1988. Organic enrichment or toxicity? A comparison of the
690 effects of kelp and crude oil in sediments on the colonization and growth of benthic
691 infauna. J. Exp. Mar. Biol. Ecol. 124: 261-282. https://doi.org/10.1016/0022-
692 0981(88)90175-X.
693 Sun, S., Hu, C., Tunnell Jr. J.W., 2015. Surface oil footprint and trajectory of the Ixtoc-1 oil spill
694 determined from Landsat/MSS and CZCS observations. Mar. Poll. Bull. 101, 643-641.
695 http://dx.doi.org/10.1016/j.marpolbul.2015.10.036.
696 Valentine, D.L, Fisher, G.B., Bagby, S.C., Nelson, R.K., Reddy, C.M., Sylva, S.P., , Woo M.A.,
697 2014. Fallout plume of submerged oil from Deepwater Horizon. Proc. Nat. Acad. Sci.
698 111(45), 15906 -15911. www.pnas.org/cgi/doi/10.1073/pnas.1414873111.
699 Vonk, S.M., Hollander, D.J., Murk, A.J., 2015. Was the extreme and wide-spread marine snow
700 sedimentation and flocculent accumulation (MOSSFA) event furing the Deepwater
701 Horizon blow-out unique? Mar. Poll. Bull. 100, 5-12.
702 http://dx.doi.org/10.1016/j.marpolbul.2015.08.023.
703 Wade, T.L., Soliman, Y., Sweet, S.T., Wolff, G.A., Presley, B.J., 2008. Trace elements and
704 polycyclic aromatic hydrocarbons (PAHs) concentrations in deep Gulf of Mexico
705 sediments. Deep-Sea Res. Part II, 55: 2585-2593.
706 https://doi.org/10.1016/j.dsr2.2008.07.006.
707 Washburn, T., Rhodes, A.C.E., Montagna, P.A., 2016. Benthic taxa as potential indicators of a
708 deep-sea oil spill. Ecol. Ind. 71, 587 - 597.
709 http://dx.doi.org/10.1016/j.ecolind.2016.07.045.
710 Washburn, T.W., Reuscher, M.G., Montagna, P.A., Cooksey, C.,Hyland, J.L., 2017.
711 Macrobenthic community structure in the deep Gulf of Mexico one year after the

712 Deepwater Horizon blowout. Deep-Sea Res. Part I 127: 21-30.
713 http://dx.doi.org/10.1016/j.dsr.2017.06.001.
714 Washburn, T.W., Demopoulos, A.W.J., Montagna, P.A., 2018. Macrobenthic infaunal
715 communities associated with deep-sea hydrocarbon seeps in the northern Gulf of Mexico.
716 Mar. Ecol. Evolut. Perspect.39, e12508. https://doi.org/10.1111/maec.12508.
717 Yáñez-Arancibia, A., Day, J.W., 2004. The Gulf of Mexico: towards an integration of coastal
718 management with large marine ecosystem management. Oce Coast. Manage. 47, 537-
719 563. https://doi.org/10.1016/j.ocecoaman.2004.12.001.
720 Ziervogel, K., McKay, L., Rhodes, B., Osburn, C.L., Dickson-Brown, J., Arnosti, C., Teske, A.,
721 2012. Microbial activities and dissolved organic matter dynamics in oil-contaminated
722 surface seawater from the Deepwater Horizon oil spill site. PloS One 7(4), e34816.
723 https://doi.org/10.1371/journal.pone.00.